Acid-sensitive ionic channels in midbrain dopamine neurons are sensitive to ammonium, which may contribute to hyperammonemia damage

Volodymyr I. Pidoplichko and John A. Dani*

Department of Neuroscience, Menninger Department of Psychiatry and Behavioral Science, and Program in Structural and Computational Biology and Molecular Biophysics, Baylor College of Medicine, Houston, TX 77030

Edited by Bertil Hille, University of Washington, Seattle, WA, and approved June 12, 2006 (received for review January 30, 2006)

Acid-sensitive ion channels (ASICs) are proton-gated and belong to the family of degenerin channels. In the mammalian nervous system, ASICs are most well known in sensory neurons, where they are involved in nociception, occurring when injury or inflammation causes acidification. ASICs also are widely expressed in the CNS, and some synaptic roles have been revealed. Because neuronal activity can produce pH changes, ASICs may respond to local acidic transients and alter the excitability of neuronal circuits more widely than is presently appreciated. Furthermore, ASICs have been found to underlie calcium transients that contribute to neuronal death. Degeneration of midbrain dopamine neurons is characteristic of advanced idiopathic Parkinson's disease. Therefore, we tested for functional ASICs in midbrain dopamine neurons of the ventral tegmental area and substantia nigra compacta. Patch-clamp electrophysiology applied to murine midbrain slices revealed abundant acid-sensitive channels. The ASICs were gated and desensitized by extracellular application of millimolar concentrations of NH_4Cl. Although the NH_4Cl solution contains micromolar concentrations of NH_3 at pH 7.4, our evidence indicates that NH_4^+ gates the ASICs. The proton-gated and the ammonium-gated currents were inhibited by tarantula venom (psalmotoxin), which is specific for the ASIC1a subtype. The results show that acid-sensitive channels are expressed in midbrain dopamine neurons and suggest that ammonium sensitivity is a widely distributed ASIC characteristic in the CNS, including the hippocampus. The ammonium sensitivity suggests a role for ASIC1s in hepatic encephalopathy, cirrhosis, and other neuronal disorders that are associated with hyperammonemia.

hepatic encephalopathy | mesolimbic dopamine | Parkinson's disease | proton gating | cirrhosis

Proton-gated channels or acid-sensitive ion channels (ASICs) are present in sensory neurons, where they have roles in nociception, taste, and possibly other modalities (1–5). Recently, six ASIC subunits were cloned (6, 7) and identified as belonging to a broad family of degenerin (Deg) channels. ASIC1a (also known as BNaC2) and ASIC1b (ASIC1β) are the splice variants of the ASIC1 gene (6, 8, 9). ASIC2a (BNaC1, MDEG) and ASIC2b (MDEG2) are the spliced forms of the ASIC2 gene (10). Other subunits are ASIC3 (DRASIC) (7, 11) and ASIC4 (SPASIC) (12, 13). The ASIC subunits form a variety of heteromeric channels in heterologous expression systems, and subunits other than ASIC2b and ASIC4 also form functional homomeric channels in expression systems (14).

Although there has been much progress, there is still uncertainty about the pharmacology, the endogenous subunit composition, and the functional significance of different CNS ASIC subtypes (4, 5, 15, 16). ASIC1 is the subunit most abundantly expressed in the mammalian brain and has been shown to be involved in synaptic plasticity (17). ASICs in the CNS also have been implicated in Ca^{2+} toxicity arising from ischemia, and inhibition or knockout of ASIC1 protected the mouse brain from ischemic acidosis (18).

Because midbrain dopamine neurons are prone to toxic damage that leads to disorders such as Parkinson's disease, we investigated the presence and characteristics of ASICs in mesolimbic dopamine neurons. In rodent midbrain slices, large pH-sensitive conductances were observed. These ASICs also were activated and desensitized by external NH_4Cl at pH 7.4. To help identify these conductances, we used a subunit-specific blocker and compared ASICs from other tissue preparations and concluded that the majority of the current arises from ASIC1-like channels. Our study demonstrates ASIC ammonium sensitivity from CNS neurons in an intact preparation, and the results are consistent with the NH_4Cl-gated currents observed in isolated sensory neurons (19). The results suggest that the main ASIC in murine dopamine neurons is an ASIC1-type ammonium-sensitive channel. The ammonium sensitivity offers the potential for ammonia and acidosis toxicity impacting dopamine neurons and suggests a general route for neuronal damage arising from hyperammonemia.

Results

Acid pH and Ammonium Gate Channels on Dopamine Neurons. Pressure application of acidified solution (pH 5.4) directly onto dopamine neurons from mouse midbrain slices elicited large currents (680 ± 110 pA, $n = 12$; mean ± SE) (Fig. 1*A*). The acid-gated currents were not inhibited by a mixture of antagonists to ionic channels gated by glutamate (20 μM 6-cyano-7-nitroquinoxaline-2,3-dione/50 μM 2-amino-5-phosphopentanoic acid), GABA (20 μM bicuculline), and acetylcholine (1 μM atropine/5 μM mecamylamine). In these experiments, voltage-gated sodium current was inhibited by extracellular tetrodotoxin (1 μM), and voltage-gated current activated by hyperpolarization (I_h current) was inhibited by intracellular QX-314 (5 mM) or tetraethylammonium (50 mM) (20, 21). The dose–response relationship for activation by protons had an apparent Hill coefficient of 1.0 and an apparent EC_{50} of pH 5.5 (Fig. 1*C*). These characteristics resemble those from homomeric ASIC1a channels (14).

Similar currents (490 ± 90 pA, $n = 5$) were also elicited by pressure application of an extracellular solution containing NH_4Cl (72 mM) at pH 7.4 (Fig. 1*B*). The gating by NH_4Cl seen in these dopamine neurons is like that previously observed from ASICs located in peripheral neurons (19). Similar acid-gated and NH_4Cl-gated currents were also observed from HEK 293 cells and hippocampal interneurons (Fig. 6, which is published as supporting information on the PNAS web site).

Conflict of interest statement: No conflicts declared.

This paper was submitted directly (Track II) to the PNAS office.

Abbreviation: ASIC, acid-sensitive ion channel.

*To whom correspondence should be addressed. E-mail: jdani@bcm.tmc.edu.

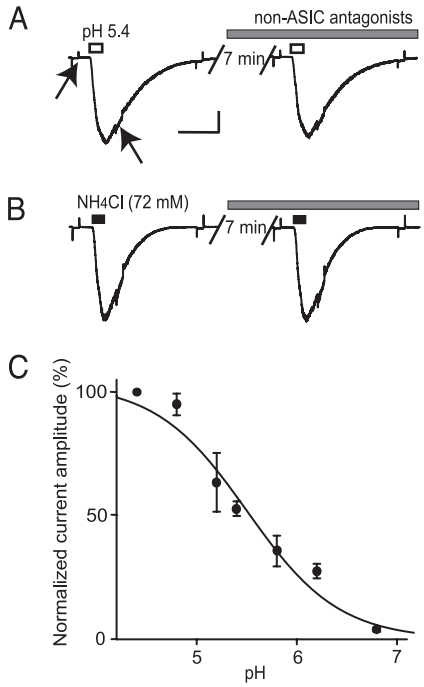

Fig. 1. Proton-gated and ammonium-gated currents from mouse midbrain dopamine neurons. (*A*) Proton-gated currents were elicited by a 300-ms pressure application of acidified (pH 5.4) extracellular solution (open bar). Acid-activated current was not inhibited by bath application of a mixture of antagonists to glutamate, GABA, and acetylcholine ligand-gated ionic channels (gray bar). Tetrodotoxin was present in the extracellular solutions to inhibit sodium currents, and 50 mM tetraethylammonium was in the internal solution to inhibit I_h current. Hyperpolarizing pulses (−10 mV for 200 ms) applied before, after, and during the agonist application indicated that the proton-gated current arose from a 5.2 ± 0.2 (mean ± SE, $n = 5$) conductance increase over baseline. The conductance increase was estimated as the ratio of the conductance close to the maximum of the ligand-gated current to the conductance at the baseline (indicated by the arrows). Calibration bars represent 1 s and 200 pA for all current traces, which were all measured at a holding potential of −65 mV. (*B*) After 23 min to wash off the antagonists, the current was evoked by pressure application of an extracellular solution containing NH_4Cl (72 mM) at pH 7.4 (black bars). The current again was not inhibited by bath application of the non-ASIC antagonists (gray bar). The NH_4Cl-gated conductance increased 5.3 ± 0.3 ($n = 4$) times over baseline. (*C*) The dose–response dependence for the acid-gated current mediated by ASICs is shown. Data points were collected at 23°C ($n = 4$) by pressure-applying the pH-altered solutions with a puffer pipette. Thus, the exact pH hitting the cell surface was not the same as the pH in the puffer pipette, because the pressure-applied solution was diluted by the bath (see ref. 24).

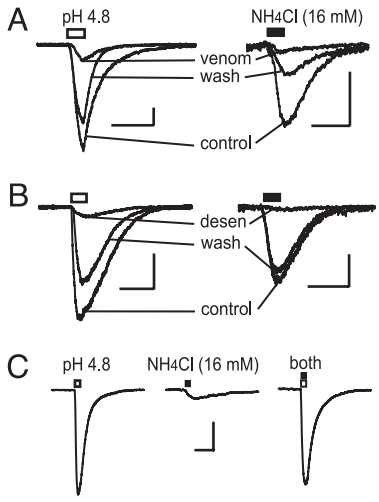

Fig. 2. Proton-gated and ammonium-gated currents are mediated by channels with common properties. (*A*) Proton-gated (pH 4.8, open bar) and NH_4Cl-gated (16 mM at pH 7.4, filled bar) currents were inhibited by *P. cambridgei* venom (1:1,000 dilution), an ASIC1a antagonist. (*B*) To test for cross-desensitization, currents activated by pressure-applied acidified solution (pH 4.8, open bar) were desensitized by bath-applied 8 mM NH_4Cl-containing solution. Likewise, currents elicited by 16 mM NH_4Cl-containing solution (filled bar) were desensitized by bath-applied solution with a pH of 6.8. Holding current was set to zero for comparison of the current traces. In *A* and *B*, the calibration bars represent 1 s and 200 pA for all current traces, and the holding potential was −65 mV. (*C*) To test for nonadditivity, pressure application of a solution at pH 4.8 (open bar, *Left*) activated a maximal current. Pressure application of 16 mM NH_4Cl to the same neuron at pH 7.4 evoked a smaller inward current (filled bar, *Center*). The current induced by the application of 16 mM NH_4Cl at pH 4.8 (open and filled bars) to the same neuron demonstrated no gain in amplitude (*Right*). Each trace is the average of three records. The calibration bars represent 1 s and 500 pA, and the holding potential was −65 mV.

Ammonium Gates ASICs from Dopamine Neurons. The venom of the tarantula species *Psalmopoeus cambridgei* is an antagonist of ASIC1a channels (22, 23). When applied at a 1:1,000 dilution, the spider venom inhibited currents activated by low pH or NH_4Cl. At 1:1,000 dilution, the venom inhibited acid-gated (pH 4.8) currents by 89 ± 2% ($n = 4$) and inhibited NH_4Cl-gated (16 mM at pH 7.4) currents by 92 ± 1% ($n = 3$) (Fig. 2*A*).

To further test whether the acid-gated and NH_4Cl-gated currents were the same entity, we examined whether acid and NH_4Cl caused cross-desensitization. Currents activated by acid (pH 4.8) were desensitized (90 ± 1% inhibition, $n = 5$) by bath-applied NH_4Cl (8 mM) (Fig. 2*B Left*). Likewise, currents activated by solution containing NH_4Cl (16 mM) were desensitized (93 ± 2% inhibition, $n = 4$) by reducing the bath pH from 7.4 to 6.8 (Fig. 2*B Right*). Similar cross-desensitization was also observed for acid-gated and NH_4Cl-gated currents from hippocampal interneurons (Fig. 6).

Maximal activation of the ASICs provided further evidence that the channels activated by acid and NH_4Cl were the same population. The ASICs were maximally activated by pressure application of an extracellular solution at pH 4.8 (Fig. 2*C Left*). Then, from the same dopamine neuron, currents were activated by a solution containing 16 mM NH_4Cl (Fig. 2*C Center*). Demonstrating nonadditivity, coapplication of a solution containing 16 mM NH_4Cl at pH 4.8 did not activate a larger current. Rather, the current activated by coapplication (Fig. 2*C Right*) was statistically the same as the maximal current activated by pH 4.8 alone ($P > 0.05$, *t* test for different populations; $n = 5$).

Finally, another characteristic of ASIC1 channels is that the amplitude of their acid-gating currents increases as the calcium concentration in the external solution decreases below biological levels (15). We found the same characteristic for these ammonium-gated currents. Currents activated by pressure-applied extracellular ammonium chloride demonstrated a >2-fold increase in amplitude when 2 mM Ca^{2+} was replaced by using a nominally Ca^{2+}-free solution to bathe the slice. The increase in amplitude was 2.4 ± 0.2 ($n = 6$) for pressure application of 16 or 32 mM NH_4Cl (Fig. 7, which is published as supporting information on the PNAS web site).

Ammonium, Not Ammonia, Gates the ASICs. The ASIC currents were activated by solutions containing NH_4Cl. At biological pH, ammonium (NH_4^+) is the main species, but there is a minor ammonia (NH_3) component. In a solution containing 16 mM NH_4Cl, there is 278 μM ammonia at pH 7.5 and 111 μM ammonia at pH 7.1. If ammonia (NH_3) were the primary component activating the ASICs, then the current would be larger at pH 7.5, but it is not (Fig. 3). We activated currents with

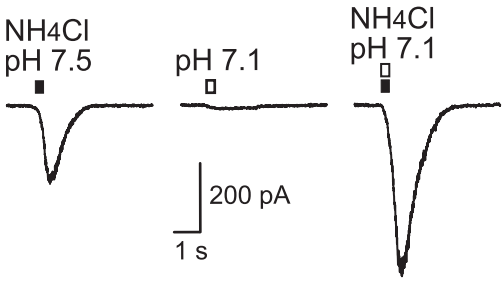

Fig. 3. Ammonium, not ammonia, gates the ASICs. Pressure application of NH_4Cl (16 mM) to a dopamine neuron at pH 7.5 (filled bar, *Left*) activated inward current. Pressure application of acidified solution (pH 7.1, open bar, *Center*) alone activated a very small current. Pressure application of 16 mM NH_4Cl at pH 7.1 (open and filled bars, *Right*), which increases the concentration of ammonium while decreasing the concentration of ammonia, to the same neuron activated a current with significantly larger amplitude. The holding potential was −65 mV. Each current trace is the average of three recordings.

a solution containing 16 mM NH_4Cl at pH 7.5 (Fig. 3 *Left*). We then demonstrated that pH 7.1 activates a barely detectable ASIC current (Fig. 3 *Center*) because this proton concentration is at the beginning of the activation dose–response curve for these currents (see Fig. 1*C*). The currents elicited in the same dopamine neurons by 16 mM NH_4Cl at pH 7.1 were 1.9 ± 0.2 ($n = 5$) times larger than at pH 7.5. Because pH does not activate an appreciable current at pH 7.1, the result indicates that the currents are gated by NH_4^+ and not by NH_3.

Dose–Response Relationship for Ammonium-Gated Currents. It is biologically important to know at what concentration ammonium evokes meaningful currents. To estimate the lower limit of the concentration dependence, we bath-applied NH_4Cl while monitoring the whole-cell currents (Fig. 4). For these experiments, we doubled the speed of bath application (8 ml/min in a 0.8-ml chamber) to synchronize the ammonium-gated currents to increase our ability to measure small currents. There were detectable currents at the lowest ammonium concentration studied, which was 1 mM, but an ammonium concentration of 4 mM produced consistently measurable currents (Fig. 4*A*). At concentrations much higher than 16 mM in the bath solution, however, the neuron being studied expressed unusual characteristics, suggesting that the cell was being damaged or that unusually large currents were developing. Therefore, after establishing the low concentration profile of the dose–response curve with bath application of NH_4Cl (Fig. 4*C*), we then used a puffer pipette to apply ammonium by pressure to the cell (24).

These puffer-pipette exposures to ammonium are brief, and the cell can survive. However, the exact concentration arriving at the cell surface is lower than in the puffer pipette and cannot be known exactly because the pressure-applied solution mixes with and is diluted by the bath solution. However, 16 mM NH_4Cl in the puffer pipette produces a consistently measurable current (Fig. 4*B*, trace 1), which suggests the result obtained with 4–8 mM NH_4Cl applied to the bath (compare Fig. 4*A*). Therefore, the concentration applied at the cell surface may be estimated by using the lowest concentrations of bath-applied NH_4Cl that activated consistently measurable currents. The puffer-pipette method gives only the approximate shape of the concentration dependence for current activation (Fig. 4*D*). Although not exact, the two methods together indicate the biologically important case accurately at the low concentrations and indicate the general shape of the dose–response relationship.

Long-Term Activation by Ammonium. Extracellular hyperammonemia leading to hepatic encephalopathy depolarizes cells by

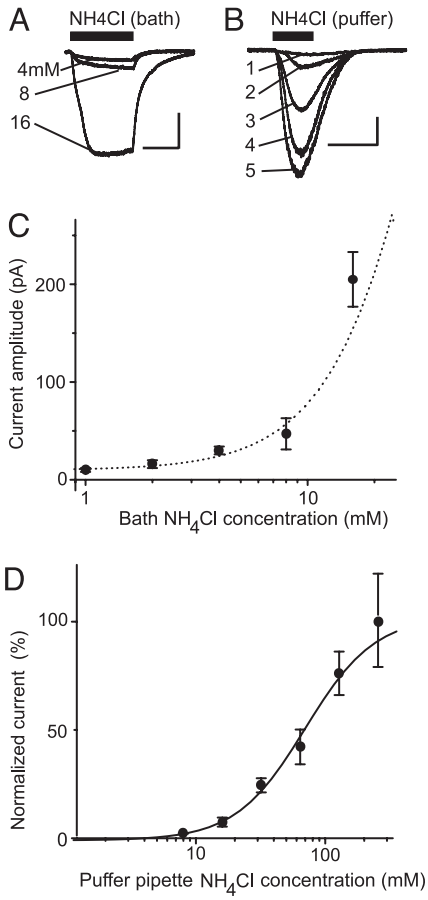

Fig. 4. Estimated minimum concentration for activation of ASICs by ammonium. (*A*) Example current traces are shown from the same cell for bath application (filled bar) of 4, 8, and 16 mM NH_4Cl. Calibration bars represent 5 min and 100 pA. (*B*) Example current traces are shown from the same cell upon pressure application by a puffer pipette containing NH_4Cl (filled bar) at the following concentrations: 16 mM (trace 1), 32 mM (trace 2), 64 mM (trace 3), 128 mM (trace 4), and 256 mM (trace 5). The actual concentration reaching the cell surface is lower than the puffer-pipette concentration. Calibration bars represent 1 s and 200 pA. (*C*) The initial part of the dose–response relationship is shown for bath-applied NH_4Cl. These currents give an accurate estimate of the lowest concentrations that activate detectable currents from dopamine neurons in this midbrain slice. Data points were averaged from 3 to 10 cells and represent the mean ± SE. (*D*) Dose–response dependence for ASIC activation by pressure-applied external NH_4Cl. The abscissa represents the concentration of NH_4Cl in the puffer pipette, but a lower concentration is reaching the cell surface. Data points were averaged from 3 to 11 cells and represent the mean ± SE. The curve (sigmoid logistic) indicates an apparent EC_{50} value of 68 mM NH_4Cl (in the puffer pipette, not on the cell surface) and the apparent Hill coefficient of 1.6. Based on the currents evoked by bath-applied NH_4Cl, we may estimate that the actual EC_{50} is closer to 20–40 mM ammonium.

means of an unknown mechanism (25). To simulate a near lethal hyperammonemic blood concentration, we tested NH_4Cl (16 mM) applied to the bath of midbrain slices while voltage-clamping (Fig. 5*A*) or current-clamping (Fig. 5 *B* and *C*) dopamine neurons. In voltage-clamp mode, bath-applied NH_4Cl (16 mM at pH 7.4) induced inward current (70 ± 20 pA, $n = 7$) measured after 15 min in ammonium chloride. The brief inward currents (downward deflections) observed on the trace are ASICs activated by brief pressure applications of acidified solution (pH 5.4 for 300 ms) delivered every 60 s. The pressure applications only apply acid to a small area of the whole cell, but the bath-applied NH_4Cl activates channels along the whole cell surface. Therefore, the bath-applied NH_4Cl desensitizes much of

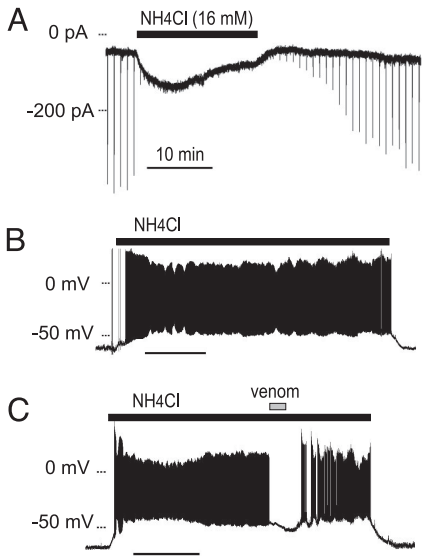

Fig. 5. Long-lasting depolarizations of dopamine neurons caused by hyperammonemia. (*A*) In voltage-clamp mode, bath-applied NH_4Cl (16 mM at pH 7.4, filled bar) induced transient and sustained inward holding current. Pressure application of extracellular acidified solution (pH 5.4; 300 ms every 60 s) induced transient currents, shown as brief downward deflections (inward current). These acid-induced currents are strongly desensitized by the bath-applied NH_4Cl. The holding potential was −65 mV. (*B*) In current-clamp mode, bath-applied NH_4Cl (16 mM at pH 7.4, filled bar) caused depolarization and evoked action potentials. (*C*) When *P. cambridgei* venom (1:1,000 dilution, gray bar), an ASIC1a antagonist, was applied during the current-clamp experiment, the depolarization was suppressed, and the spiking stopped. After wash-out of the venom, the depolarization and spiking resumed. During all of these experiments, glutamate receptors were inhibited by kynurenic acid (1 mM), GABAa receptors were inhibited by bicuculline (20 μM), and muscarinic receptors were inhibited by atropine (1 μM) in the extracellular solution. (Scale bars: 10 min.)

the transient acid-gated current, but a portion of the ASICs continue to mediate current during the entire time that NH_4Cl is present.

In current-clamp mode, bath-applied NH_4Cl (16 mM at pH 7.4 for 40 min) induced a slowly developing depolarization (22 ± 2 mV, $n = 4$) that caused the dopamine neurons to fire action potentials that continued while the NH_4Cl was present (Fig. 5*B*). To verify that the depolarization and the firing of action potentials were mediated by ASICs, we applied spider venom ($n = 2$) during the bath application of NH_4Cl (16 mM). Application of the venom inhibited the sustained depolarization and stopped the ongoing action potentials (Fig. 5*C*).

Discussion

We demonstrated large acid-gated currents in midbrain dopamine neurons and in hippocampal interneurons (Fig. 6) and revealed the ammonium sensitivity of these ASICs. The acid-gated currents were desensitized by ammonium, and, likewise, the ammonium-gated currents were desensitized by acidified solutions. Although desensitizing currents gated by external NH_4Cl have been previously observed in sensory neurons (26) and *Xenopus* oocytes (27), acid activation and ammonium activation have only previously been linked in rat trigeminal ganglion neurons (19), not in the CNS.

Inhibition by the specific ASIC1a antagonist psalmotoxin (23), the pH dependence for activation (14), and the calcium modulation of current amplitudes (15) suggest that the acid-gated and ammonium-gated currents from midbrain dopamine neurons are mediated by the ASIC1 subtype. This conclusion is supported by the acid-gated and ammonium-gated currents found in HEK 293 cells, which endogenously express only the ASIC1 subunit (28) (see Fig. 6). Immunohistochemical methods also have shown that the ASIC1 subtype is the predominant subtype in the hippocampus and the midbrain (29). These cumulative data support that ASIC1s are also ammonium-gated channels.

CNS cellular mechanisms of ammonia (ammonium) toxicity remain largely unknown, and the potential importance of ammonium-sensitive ASICs is presently unappreciated in the literature. ASIC1 is calcium permeable (30) and can produce calcium-dependent neuronal death (18). As we demonstrated in Fig. 5, ammonium is capable of inducing long-lasting currents. Thus, even small, long-lasting currents could significantly alter the ionic composition of the cytoplasm and influence the cell's electrical and enzymatic properties. In addition, we observed in our patch-clamp experiments that higher concentrations of ammonium caused large currents with unusual characteristics that suggested that the cell was being damaged. Thus, ammonium-sensitive ASICs may participate in the pathological conditions of the brain caused by elevated blood ammonium content arising from cirrhosis or hepatic failure (31–35).

Normally, free ammonia levels in blood are <40 μM, which corresponds to 3 mM NH_4Cl at pH 7.4 (36, 37). Our results indicate that this concentration of ammonium begins to induce detectable current by means of ASIC1. During pathological conditions, ammonium levels can be substantially higher, and persistent blood content equivalent to 16 mM NH_4Cl (220 μM NH_3 at pH 7.4) may lead to death (36). Free ammonia levels in blood correlate with the severity of hepatic encephalopathy symptoms (38). It has been reported, however, that transient free ammonia blood levels between 100 and 300 μM (22 mM NH_4^+) were not lethal in children with hyperammonemia (37). Our evidence showing that elevated ammonium can produce prolonged depolarization and neuronal firing suggests it is reasonable to hypothesize that ammonium-gated ASICs could contribute to toxicity during pathologies that elevate ammonium.

Hyperammonemia ensues during hepatic encephalopathy, which is characterized by a progressive and diffuse impairment in brain function. In some patients, parkinsonian symptoms arise in association with basal ganglia alterations, including altered dopamine neurotransmission (39, 40). Because dopamine neurons of the midbrain are particularly sensitive to toxic cell death, they might be vulnerable to elevated ammonium concentrations by means of ammonium-sensitive ASIC1s.

There also are other examples where the ammonium sensitivity of the ASICs may have a contributing role. We demonstrated ammonium-gated ASIC current in the hippocampus, and those currents may contribute to the hepatic encephalopathy-related impairment reported in hippocampal circuits (41, 42). ASIC1 mRNA also has been identified in normal human astrocytes (43), making these channels potential sites of action for the gliosis observed during hyperammonemic conditions (44).

Elevated concentrations of ammonium arising during pathology will affect all cells expressing ammonium-sensitive ASICs and will likely influence circuit activity in many neuronal networks if sufficiently high ammonium concentrations are achieved. It is important to recall, however, that widely distributed ASICs are likely to serve normally in a neuromodulatory role as they respond to activity-dependent local pH (and ammonium) changes.

Materials and Methods

The experiments were conducted by using horizontal brain slices cut from C57 mice to contain the hippocampus and the ventral tegmental area and substantia nigra compacta of the midbrain. The slice preparation, solutions, and pressure application of solutions are described in refs. 24, 45, and 46. The bath solution was as follows (in mM): 128 NaCl/2.5 KCl/1.25 NaH_2PO_4/21

$NaHCO_3$/2–2.5 $CaCl_2$/1 $MgCl_2$/25 D-glucose, pH 7.4. Patch electrodes had resistances of 3–5 megaohms and were filled with the following internal solution (in mM): 60 $CsCH_3SO_3$/60 KCH_3SO_3/10 KCl/10 EGTA/10 Hepes/5 Mg-ATP/0.3 Na_3GTP, pH 7.2.

The external solutions for pressure application had an ionic composition similar to the bath solution but were buffered by 20 mM Hepes. To obtain NH_4Cl-containing solutions (e.g., for the dose–response relationship), the sodium-based solution was mixed with one containing 128 mM NH_4Cl instead of NaCl. NH_4Cl replaced NaCl on an equimolar basis by mixing the two solutions. Hypertonic 256 mM NH_4Cl solution was also used in some pressure-application experiments. In the experiments in which bath application of ammonium-containing solutions was used, the conventional flow rate of the bath (4 ml/min) was doubled. The experimental chamber volume was ≈0.8 ml. The osmolarity of conventional solutions was adjusted by D-glucose. As a control, pressure application of the external solution without agonists elicited no measurable artifacts.

To ensure that the currents were mediated by ASICs, we inhibited many other ion channels with the following compounds in the bath: 6-cyano-7-nitroquinoxaline-2,3-dione- (20 μM) or kynurenic acid (1 mM)-inhibited non-NMDA glutamate receptors, 2-amino-5-phosphopentanoic acid (50 μM)-inhibited NMDA glutamate receptors, bicuculline (20 μM)-inhibited GABAa receptors, atropine (1 μM) nonselectively inhibited muscarinic acetylcholine (ACh) receptors, and mecamylamine (5 μM) nonselectively inhibited nicotinic ACh receptors. In some experiments, extracellular tetrodotoxin (1 μM) or intracellular QX-314 (5 mM) inhibited voltage-gated sodium currents. Dopamine neurons in the midbrain were identified based on their location, general anatomy, and large I_h currents, as described in refs. 46–50. Intracellular tetraethylammonium (50 mM) was used to block current activated by hyperpolarization (I_h) in some experiments (20). All chemicals were purchased from Sigma (St. Louis, MO). *P. cambridgei* venom ("neat venom") was obtained from Spider Pharm (Yarnell, AZ). The experiments were performed at room temperature of 23 ± 1°C.

We thank Dr. Michael Krause for valuable comments on the manuscript. This work was supported by National Institute of Neurological Disorders and Stroke Grants NS21229 and NS048505 and National Institute on Drug Abuse Grant DA09411.

1. Krishtal, O. A. & Pidoplichko, V. I. (1980) *Neuroscience* **5,** 2325–2327.
2. Krishtal, O. A. & Pidoplichko, V. I. (1981) *Neuroscience* **6,** 2599–2601.
3. Krishtal, O. A. & Pidoplichko, V. I. (1981) *Neurosci. Lett.* **24,** 243–246.
4. McCleskey, E. W. & Gold, M. S. (1999) *Annu. Rev. Physiol.* **61,** 835–856.
5. Waldmann, R. (2001) *Adv. Exp. Med. Biol.* **502,** 293–304.
6. Waldmann, R., Champigny, G., Bassilana, F., Heurteaux, C. & Lazdunski, M. (1997) *Nature* **386,** 173–177.
7. Waldmann, R., Bassilana, F., de Weille, J., Champigny, G., Heurteaux, C. & Lazdunski, M. (1997) *J. Biol. Chem.* **272,** 20975–20978.
8. Chen, C. C., England, S., Akopian, A. N. & Wood, J. N. (1998) *Proc. Natl. Acad. Sci. USA* **95,** 10240–10245.
9. Bassler, E. L., Ngo-Anh, T. J., Geisler, H. S., Ruppersberg, J. P. & Grunder, S. (2001) *J. Biol. Chem.* **276,** 33782–33787.
10. Lingueglia, E., de Weille, J. R., Bassilana, F., Heurteaux, C., Sakai, H., Waldmann, R. & Lazdunski, M. (1997) *J. Biol. Chem.* **272,** 29778–29783.
11. Babinski, K., Le, K. T. & Seguela, P. (1999) *J. Neurochem.* **72,** 51–57.
12. Akopian, A. N., Chen, C. C., Ding, Y., Cesare, P. & Wood, J. N. (2000) *NeuroReport* **11,** 2217–2222.
13. Grunder, S., Geissler, H. S., Bassler, E. L. & Ruppersberg, J. P. (2000) *NeuroReport* **11,** 1607–1611.
14. Hesselager, M., Timmermann, D. B. & Ahring, P. K. (2004) *J. Biol. Chem.* **279,** 11006–11015.
15. Sutherland, S. P., Cook, S. P. & McCleskey, E. W. (2000) *Prog. Brain Res.* **129,** 21–38.
16. Kellenberger, S. & Schild, L. (2002) *Physiol. Rev.* **82,** 735–767.
17. Wemmie, J. A., Chen, J., Askwith, C. C., Hruska-Hageman, A. M., Price, M. P., Nolan, B. C., Yoder, P. G., Lamani, E., Hoshi, T., Freeman, J. H., Jr., & Welsh, M. J. (2002) *Neuron* **34,** 463–477.
18. Xiong, Z. G., Zhu, X. M., Chu, X. P., Minami, M., Hey, J., Wei, W. L., MacDonald, J. F., Wemmie, J. A., Price, M. P., Welsh, M. J. & Simon, R. P. (2004) *Cell* **118,** 687–698.
19. Pidoplichko, V. I. (1992) *Gen. Physiol. Biophys.* **11,** 39–48.
20. Budde, T., White, J. A. & Kay, A. R. (1994) *J. Neurophysiol.* **72,** 2737–2742.
21. Kilb, W. & Luhmann, H. J. (2000) *J. Neurophysiol.* **84,** 1681–1691.
22. Escoubas, P., De Weille, J. R., Lecoq, A., Diochot, S., Waldmann, R., Champigny, G., Moinier, D., Menez, A. & Lazdunski, M. (2000) *J. Biol. Chem.* **275,** 25116–25121.
23. Gitterman, D. P., Wilson, J. & Randall, A. D. (2005) *J. Physiol. (London)* **562,** 759–769.
24. Pidoplichko, V. I. & Dani, J. A. (2005) *J. Neurosci. Methods* **142,** 55–66.
25. Szerb, J. C. & Butterworth, R. F. (1992) *Prog. Neurobiol.* **39,** 135–153.
26. Mironov, S. L. & Lux, H. D. (1993) *NeuroReport* **4,** 1055–1058.
27. Burckhardt, B. C. & Burckhardt, G. (1997) *Pflügers Arch.* **434,** 306–312.
28. Gunthorpe, M. J., Smith, G. D., Davis, J. B. & Randall, A. D. (2001) *Pflügers Arch.* **442,** 668–674.
29. Alvarez de la Rosa, D., Krueger, S. R., Kolar, A., Shao, D., Fitzsimonds, R. M. & Canessa, C. M. (2003) *J. Physiol. (London)* **546,** 77–87.
30. Yermolaieva, O., Leonard, A. S., Schnizler, M. K., Abboud, F. M. & Welsh, M. J. (2004) *Proc. Natl. Acad. Sci. USA* **101,** 6752–6757.
31. Raabe, W. (1993) *Adv. Exp. Med. Biol.* **341,** 71–82.
32. Mousseau, D. D. & Butterworth, R. F. (1994) *Proc. Soc. Exp. Biol. Med.* **206,** 329–344.
33. Menkes, J. H. (1995) in *Textbook of Child Neurology* (Williams & Wilkins, Baltimore), pp. 1–199.
34. Hazell, A. S. & Butterworth, R. F. (1999) *Proc. Soc. Exp. Biol. Med.* **222,** 99–112.
35. Butterworth, R. F. (2002) *Metab. Brain Dis.* **17,** 221–227.
36. Lockwood, A. H., Yap, E. W. & Wong, W. H. (1991) *J. Cereb. Blood Flow Metab.* **11,** 337–341.
37. Kitaura, J., Miki, Y., Kato, H., Sakakihara, Y. & Yanagisawa, M. (1999) *Eur. J. Pediatr.* **158,** 410–413.
38. Ong, J. P., Aggarwal, A., Krieger, D., Easley, K. A., Karafa, M. T., Van Lente, F., Arroliga, A. C. & Mullen, K. D. (2003) *Am. J. Med.* **114,** 188–193.
39. Spahr, L., Vingerhoets, F., Lazeyras, F., Delavelle, J., DuPasquier, R., Giostra, E., Mentha, G., Terrier, F. & Hadengue, A. (2000) *Gastroenterology* **119,** 774–781.
40. Spahr, L., Burkhard, P. R., Grotzsch, H. & Hadengue, A. (2002) *Metab. Brain Dis.* **17,** 399–413.
41. Aguilar, M. A., Minarro, J. & Felipo, V. (2000) *Exp. Neurol.* **161,** 704–713.
42. Munoz, M. D., Monfort, P., Gaztelu, J. M. & Felipo, V. (2000) *Neurochem. Res.* **25,** 437–441.
43. Bubien, J. K., Ji, H. L., Gillespie, G. Y., Fuller, C. M., Markert, J. M., Mapstone, T. B. & Benos, D. J. (2004) *Am. J. Physiol.* **287,** C1282–C1291.
44. Butterworth, R. F. (2003) *J. Hepatol.* **39,** 278–285.
45. Wooltorton, J. R., Pidoplichko, V. I., Broide, R. S. & Dani, J. A. (2003) *J. Neurosci.* **23,** 3176–3185.
46. Pidoplichko, V. I., Noguchi, J., Areola, O. O., Liang, Y., Peterson, J., Zhang, T. & Dani, J. A. (2004) *Learn. Mem.* **11,** 60–69.
47. Hausser, M., Stuart, G., Racca, C. & Sakmann, B. (1995) *Neuron* **15,** 637–647.
48. Mercuri, N. B., Bonci, A., Calabresi, P., Stefani, A. & Bernardi, G. (1995) *Eur. J. Neurosci.* **7,** 462–469.
49. Pidoplichko, V. I., DeBiasi, M., Williams, J. T. & Dani, J. A. (1997) *Nature* **390,** 401–404.
50. Bonci, A. & Malenka, R. C. (1999) *J. Neurosci.* **19,** 3723–3730.